

Interplanetary Radiation and Internal Charging Environment Models for Solar Sails

Joseph I. Minow
NASA, Marshall Space Flight Center, Huntsville, AL 35812

Richard L. Altstatt and Linda Neergaard Parker
Jacobs Sverdrup, MSFC Group, Huntsville, AL 35812

Abstract

A Solar Sail Radiation Environment (SSRE) model has been developed for defining charged particle environments over an energy range from 0.01 keV to 1 MeV for hydrogen ions, helium ions, and electrons. The SSRE model provides the free field charged particle environment required for characterizing energy deposition per unit mass, charge deposition, and dose rate dependent conductivity processes required to evaluate radiation dose and internal (bulk) charging processes in the solar sail membrane in interplanetary space. Solar wind and energetic particle measurements from instruments aboard the Ulysses spacecraft in a solar, near-polar orbit provide the particle data over a range of heliospheric latitudes used to derive the environment that can be used for radiation and charging environments for both high inclination 0.5 AU Solar Polar Imager mission and the 1.0 AU L1 solar sail missions. This paper describes the techniques used to model comprehensive electron, proton, and helium spectra over the range of particle energies of significance to energy and charge deposition in thin (<25 μm) solar sail materials.

1.0 Introduction

Materials exposed to space radiation environments degrade due to the accumulation of displacement damage and dissociation of chemical bonds produced by passage of charged particles through the material. Significant localized damage can also occur due to electrostatic discharging, arcing, and treeing processes when electric fields generated by accumulated charge densities exceed the dielectric strength of the material. Evaluation of radiation susceptibility and risks of damage due to arcing for candidate solar sail materials require radiation environment models for establishing laboratory tests of radiation induced changes in material properties, modeling of radiation dose as a function of depth in materials, and modeling of the charging process.

This paper describes development of the current version (Revision A) of the Solar Sail Radiation Environment (SSRE) model developed to characterize solar wind and energetic particle (electron, proton, and helium) contributions to mission accumulated dose and internal charging over an energy range $0.01\text{keV} < E < 1\text{ MeV}$. SSRE provides environments for Solar Polar Imager's planned 0.5 astronomical unit (AU) solar polar orbit and the proposed ~1.0 AU first Lagrange point (L1) solar sail missions (L1 Diamond and Solar Sentinel missions).

2.0 Data and Model Construction

Solar wind and energetic particle instruments aboard the Ulysses spacecraft provide the approximately 12.6 years of solar wind and energetic charged particle data used to derive the radiation environment. Ulysses is the only spacecraft to sample high latitude solar wind environments far from the ecliptic plane and is therefore uniquely capable of providing the information necessary for defining radiation environments for the Solar Polar Imager spacecraft. The Solar Wind Observations Over the Poles of the Sun (SWOOPS) instrument [Bame *et al.*, 1992] provides the low energy electron and ion component of the solar wind and the Low-Energy Magnetic Spectrometer (LEMS) and Low Energy Foil Spectrometer (LEFS) instruments from the Ulysses Heliosphere Instrument for Spectra, Composition, and Anisotropy and Low Energies (HISCAL) experiment [Hunt-Ward and Armstrong, 2003] provide ion and electron environments at energies from a few 10's keV to a few MeV are used to derive the environment. Data used in the radiation model are one hour averages of appropriate plasma moments and energetic particle flux interpolated to a uniform time base.

Thermal particle populations (i=electron, proton, and helium) are modeled by Maxwellian velocity distribution functions

$$f_{M,i}(\mathbf{v}) = \frac{n_i}{(\sqrt{\pi}\theta_{M,i})^3} \exp\left[-\frac{|\mathbf{v} - \mathbf{v}_c|^2}{\theta_{M,i}^2}\right]; \quad \theta_{M,i} = \sqrt{\frac{2k_B T_i}{m_i}} \quad (1)$$

where the constants k_B and m_i are Boltzman's constant and the mass of the particle of species i , respectively. Non-thermal particle populations are modeled with Kappa velocity distributions

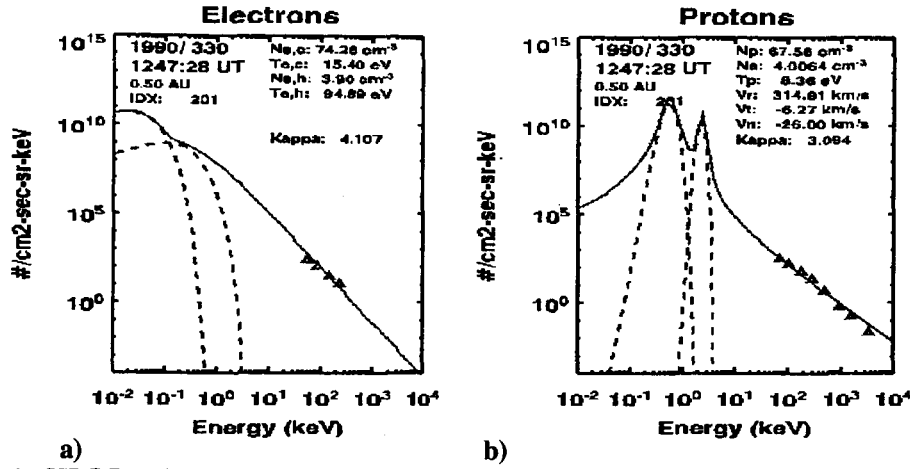


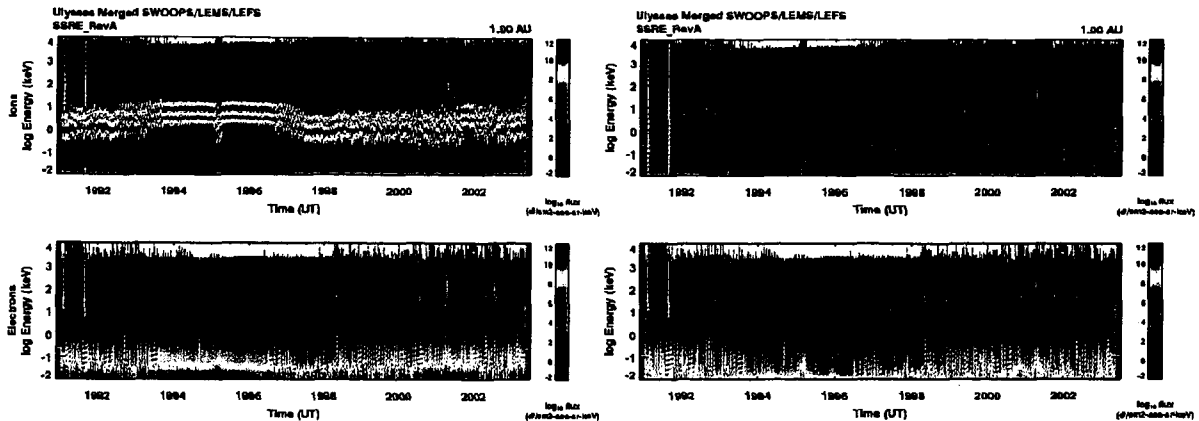
Figure 1. SSRE-Rev. A Reconstructed Energy Spectra. (a) The SSRE model (green) sums a Maxwellian core (blue) with a Kappa representation of the halo constrained by the energetic electron flux (red triangles). The Maxwellian halo representation is shown (red) for comparison. (b) Ion populations are modeled (green) as a sum of Kappa proton and helium ion distributions. Individual Maxwellian proton (dashed blue) and helium (dashed red) spectra are shown with the energetic proton flux (red triangles).

$$f_{\kappa,i}(\mathbf{v}) = \frac{n_i}{(\sqrt{\pi}\theta_{\kappa,i})^3} \frac{\Gamma(\kappa_i + 1)}{\sqrt{\kappa_i^3} \Gamma(\kappa_i - \frac{1}{2})} \left[1 + \frac{|\mathbf{v} - \mathbf{V}_c|^2}{\kappa_i \theta_{\kappa,i}^2} \right]^{-(\kappa_i + 1)} ; \theta_{\kappa,i} = \sqrt{\frac{(2\kappa - 3)k_B T_i}{\kappa_i m_i}} \quad (2)$$

where the $\kappa > 3/2$. Differential flux J_i is obtained from velocity distribution functions using $J_i = (v^2/m_i) f_i$.

Non-Maxwellian solar wind electron distribution functions [Montgomery *et al.*, 1968; Ogilvie *et al.*, 1971; Feldman *et al.*, 1975] are often represented as a superposition of three populations. A high electron density (N_e), low temperature (T_e) Maxwellian core population dominates at energies ≤ 60 eV and a Maxwellian halo population with reduced N_e and higher T_e extends to energies of $\sim 10^2$ eV. An additional “super-halo” power law population extending from ~ 1 keV to $\sim 10^2$ keV exists at the highest energies [e.g., Feldman *et al.*, 1975; Pilipp *et al.*, 1987; Larson *et al.*, 1996; Lin *et al.*, 1997]. Alternatively, Kappa distribution functions can be used to represent all three environments [Scudder, 1992; Maksimovic *et al.*, 1997; Meyer-Vernet and Issautier, 1998]. Figure 1a shows the combined approach used in construction of the SSRE electron differential flux spectra. A Maxwellian core distribution function (blue line) is added to a Kappa velocity distribution function (green line) representation for the halo and “super-halo” components of the electron population. Distribution functions are computed from SWOOPS core $N_{e,c}$, $T_{e,c}$ and halo $N_{e,h}$, $T_{e,h}$ parameters and the radial component V_r of the solar wind convection velocity V_c . Electron κ parameters are obtained by adjusting the value of κ until the reconstructed differential flux matches the LEMS and LEFS differential electron flux measurements (red triangles in Figure 1a). Electron populations are treated as isotropic at energies greater than $\sim 10^2$ keV. Asymmetric electron distributions due to the field aligned electron strahl component and temperature anisotropies with respect to the magnetic field [Fitzenreiter *et al.*, 1998] are not treated in this version of the engineering model.

Approximately 95% to 97% of the solar wind ions are protons with helium contributing only 3% to 5% to the ion number density. Other heavy ions present in the solar wind (including carbon, nitrogen, oxygen, neon, magnesium, silicon, and iron) only account for $\sim 1\%$ (or less) of the total composition of solar wind ions [Ogilvie and Coplan, 1995] and have therefore been neglected in the SSRE model environment. Proton and minor solar wind ion species typically exhibit non-thermal tails attached to a cold Maxwellian core ion population [Neugebauer and Snyder, 1966; Gloeckler *et al.*, 1992; Chotoo *et al.*, 1998]. SSRE differential ion flux spectra (Figure 1b) are constructed from Kappa distribution functions for both ion species using SWOOPS proton density N_{H^+} , proton temperature T_{H^+} , and helium density $N_{He^{++}}$. SWOOPS moments provide T_{large} and T_{small} estimates of the proton temperature computed from two different algorithms [NSSDC/2004]. The T_{large} value, which is used for the SSRE model, is derived from integrating proton distribution functions in three-dimensional velocity space over all energy channels and angle bins. T_{large} may yield overestimates of the proton temperature for cold solar wind flows so the choice of using T_{large} provides a conservative, high flux estimate in those special conditions. SWOOPS moments do not include helium temperatures so the assumption $T_{He^{++}} \approx T_{H^+}$ is used to derive helium differential flux. Components



a) **Figure 2. SSRE-Rev A 1.0 AU Flux Environments.** Differential ion (top panels) and electron (bottom panels) flux environments (a) in the direction of the solar wind flow and (b) opposite the solar wind flow. The reconstructed Ulysses environments are derived from merged solar wind plasma and energetic particle observations scaled from the spacecraft location to 1 AU.

of a single solar wind convection velocity $V_c = V_r \mathbf{r} + V_t \mathbf{t} + V_n \mathbf{n}$ is reported for all ion and electron species in the heliocentric radial, tangential, normal (RTN) coordinate system. Only the radial component V_r is used in the model because the tangential and normal components are typically small compared to the radial component of the solar wind flow. The proton κ parameter is obtained by adjusting κ to constrain the computed differential proton flux to match the measured LEMS30 and LEM120 energetic proton flux measurements (red triangles in Figure 1b). The κ parameter derived from the proton moments and energetic proton flux is simply adopted for the helium environment as well.

The radius of the Ulysses spacecraft orbit varies over a range of distances from approximately 1.0 AU to 5.4 AU from the Sun (approximately 1.3 AU to 5.4 after Jupiter fly-by in 1992) so the solar wind samples obtained by Ulysses are always from radial distances from the Sun greater than the proposed Solar Polar Imager 0.5 AU or L1, sub-L1 missions at approximately 1.0 AU. Cold plasma data has therefore been scaled from the spacecraft location to the 0.5 AU Solar Polar Imager orbit or ~ 1.0 AU L1 location using $1/r^n$ scaling laws where $n = 2.00$ for electron and ion densities, $n = 0.57$ for ion temperatures, and $n = 0.30$ for electron temperatures, and solar wind velocity is nearly independent of radial distance beyond ~ 0.3 AU to 0.5 AU [c.f., *Hundhausen, 1972; Burlaga, 1995*]. Energetic ion, electron differential flux measurements from LEMS, LEFS instruments have not been rescaled. SSRE-Rev. A is applicable for both the Solar Polar Imager and the Solar Sentinels radiation environments since the 0.5 AU environment defines the most stressing (high flux) case for both missions and 1.0 AU flux environments are reduced by only a factor of approximately four.

Using the process described above, individual differential flux spectra for an appropriate radial distance from the Sun (0.5 AU or 1.0 AU) are computed over a range of energies $0.01 \text{ keV} < E < 10 \text{ MeV}$ in 73 energy steps for each set of the one hour averaged electron and ion records yielding a set of 110,572 hourly records over a 12.6 year period. The reconstructed Ulysses solar wind differential electron and ion flux environment shown in Figure 2 is the basis of the SSRE model. The format of the plot is Universal time (in decimal years) on the horizontal axis, particle kinetic energy on the vertical axis, and differential flux intensity indicated by the color scale where flux values less than the $1.0 \times 10^2 \text{ #/cm}^2\text{-s-sr-keV}$ minimum threshold are set to white.

The model includes both flux environments impacting the illuminated side of the sail computed from the radial component of the solar wind flow (Figure 2a) and flux environments in the direction opposite the solar wind flow impacting the dark side of the sail (Figure 2b). The ion environment flowing toward the Sun (impacting the dark side of the sail) is much reduced from that observed in the direction of the solar wind flow. However, the electron environment is nearly the same in both directions, particularly at energies greater than approximately 0.1 keV where the halo electron population in the SSRE-RevA model is nearly isotropic.

It is important to note that the SSRE-RevA model provides only the free field charged particle environment and differential flux environments near the sail may be modified by the presence of photoelectrons and the Solar Sail potential due to spacecraft charging effects. Significant fluxes of photoelectrons emitted from the sail should only extend to energies of 60 eV to 100 eV and perturbations of the solar wind plasma by anticipated solar sail potentials

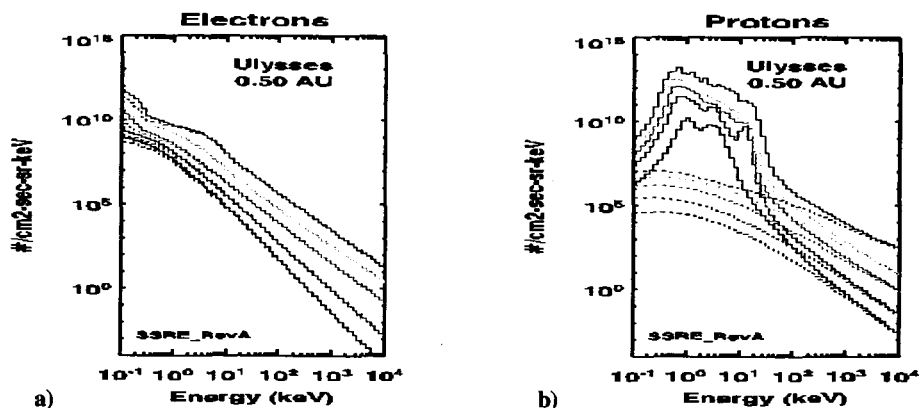


Figure 3. SSRE-Rev. A Differential Statistical Flux Environments. (a) Electron and (b) ion differential flux from energies of 0.1 keV to 1 MeV. Color coding indicates the 50% (black), 90% (blue), 95% (green), 99% (orange), and maximum (red) flux environments. Differential flux to a surface in the direction (opposite) of the solar wind flow is indicated by the solid (dotted) lines.

of tens of volts should only impact solar wind particles at energies on the order of tens of electron volts or less. Therefore, use of the environment for radiation testing at energies on the order of 1 keV and greater should be acceptable without considering charging effects and the photoelectron environment. The model provides fluence and statistical differential flux and directional flux to a surface for both the radial outward solar wind flow and flux moving radially inwards towards the Sun. The radial outward solar wind flow is used for characterizing the low energy radiation environment impact the illuminated surface of the solar sail while the radial inward solar wind flow provides the charged particle impact on the dark side of the solar sail.

3.0 Discussion

One application of the model is computation of a statistical flux spectrum from the reconstructed spectra by sorting differential flux within individual energy bins into monotonically increasing flux values and extracting the flux value which occurs N% of the way through the file where N%=50%, 90%, 95%, 99%, and 100%. The final 100% value represents the maximum flux occurring in the record. Computing the percentile flux values for each energy bin yields a statistical flux as a function of energy for each of the percentile values. Figure 3 provides statistical electron and ion differential flux in both the direction of the solar wind (solid lines) and the direction opposite the solar wind (dotted line). There is little difference in the electron environment for the two directions since the electron thermal energy dominates the energy associated with the convective motion of the plasma. Differences between the two environments are only apparent at the energies less than 1 keV. The “shoulder” in the electron spectra from 0.1 keV to 0.5 keV is due to contributions from the Maxwellian core electron population during periods of high solar wind velocity and the second “shoulder” from 1-10 keV is due to the peak in the Kappa distribution representing the halo electron population.

Ion environments are fundamentally anisotropic since the mean radial component of the solar wind convective motion is approximately 468 km/sec [Feldman *et al.*, 1977] which dominates thermal velocities which are typically only 30-60 km/sec. Multiple peaks occur in the statistical ion environment due to the effects of high and low speed solar wind environments and contributions from the multiple ion species. The peak with the highest flux in the 50% and 90% environments in particular is due to low speed solar wind protons and the secondary peak is likely a combination of both high speed protons and low speed helium ions. The third peak at energies of 10 keV to 20 keV is due to helium ions in the high speed solar wind.

The statistical flux spectra shown in Figure 3 is a technique for evaluating mean and extreme environments appropriate for time dependent phenomenon associated with dose rate effects such as radiation induced conductivity associated with internal charging analyses. Radiation environments for estimating total ionizing dose as a function of depth in the solar sail material require fluence (time integrated flux) and are best obtained by integrating the reconstructed flux environments directly over an appropriate period of time. While it may be tempting to derive a mean fluence environment for use in radiation dose analyses by adopting, for example, the 50% statistical flux and multiplying by the appropriate length of time, this approach will underestimate the real fluence, particularly at high energies.

4.0 Summary

A charged particle environment has been developed for use in evaluating radiation and charging issues for thin solar sail materials in interplanetary space. The model is based on Ulysses spacecraft observations of solar wind environments over a 12.6 year period. Electron and ion environments are provided for radially outward flowing solar wind which impacts the illuminated surface of a solar sail as well as the component of the environment impacting the dark side of the sail.

Acknowledgements

SWOOPS and HISCALE data was provided by the National Space Science Data Center courtesy of the Ulysses science team. This work was funded by the In Space Propulsion Program at Marshall Space Flight Center.

References

- Bame, S.J., D.J. McComas, B.L. Barraclough, J.L. Phillips, K.J. Sofaly, J.C. Chavez, B.E. Goldstein, R.K. Sakurai, The Ulysses Solar Wind Plasma Experiment, *Astronomy and Astrophysics, Supplement Series*, Ulysses Instruments Special Issue, Vol. 92, 237 – 265, 1992.
- Burlaga, L.F., *Interplanetary Magnetohydrodynamics*, Oxford University Press, 1995.
- Feldman, W.C., et al., Solar wind electrons, *J. Geophys. Res.*, 80, 4181 – 4196, 1975.
- Feldman W.C., J.R. Asbridge, S.J. Bame, and J.T. Gosling, Plasma and Magnetic Fields from the Sun, in *The Solar Output and its Variation*, (ed.) Oran R. White, Colorado Associated University Press, Boulder, 1977.
- Fitzenreiter, R.J., K.W. Ogilvie, D.J. Chornay, and J. Keller, Observations of electron velocity distribution functions in the solar wind by the WIND spacecraft: High angular resolution strahl measurements, *Geophys. Res. Lett.*, 25, 249-252, 1998.
- Gloeckler, G., et al., The solar wind ion composition spectrometer, *Astron. Astrophys. Suppl. Ser.*, 92, 267, 1992.
- Hundhausen, A.J., *Coronal Expansion and Solar Wind*, Springer-Verlag, 1972.
- Hunt-Ward, T., and T.P. Armstrong, Ulysses HISCALE Data Analysis Handbook, Fundamental Technologies, 2003, (<http://hiscale.ftecs.com/uly-handbk-oview.html>, accessed Aug 2004).
- Larson, D.E., R.P. Lin, K.A. Anderson, S. Ashford, C.W. Carlson, D. Curtis, R.E. Ergun, J.P. McFadden, M. McCarthy, G.K. Parks, H. Reme, J. M. Bosqued, J. Coutelier, F. Cotin, C. d'Uston, K.P. Wenzel, T.R. Sanderson, J. Henrion, and J.C. Ronnet, *Solar Wind 8 Conf. Proc.*, submitted (1996).
- Lin, R.P., D.E. Larson, R.E. Ergun, J.P. McFadden, C.W. Carlson, T.D. Phan, S. Ashford, K.A. Anderson, M. McCarthy, R. Skoug, G.K. Parks, H. Reme, J.M. Bosqued, C. d'Uston, T.R. Sanderson, and K.-P. Wenzel, Observations of the solar wind, the bow shock, and upstream particles with the Wind 3D plasma instrument, *Adv. Space Res.*, 20, Issues 4 & 5, 645-654, 1997.
- Maksimovic, M., V. Pierrard, and P. Riley, Ulysses electron distributions fitted with Kappa functions, *Geophys. Res. Lett.*, 24, 1151 – 1154, 1997.
- Meyer-Vernet, N., and K. Issautier, Electron temperature in the solar wind: Generic radial variation from kinetic collisionless models, *J. Geophys. Res.*, 103, 29,705-29,718, 1998.
- Montgomery, M.D., S.J. Bame, and A.J. Hundhausen, Solar-wind electrons: Vela 4 measurements, *J. Geophys. Res.*, 73, 4999, 1968;
- Neugebauer, M., and C.W. Snyder, Mariner 2 observations of the solar wind, *J. Geophys. Res.*, 71, 4469, 1966.
- NSSDC/2004, NSSDC Users Guide for Data from the Ulysses SWOOPS Plasma Experiment: the positive Ion experiment, (<http://helio.estec.esa.nl/ulysses/ftp/data/swoops/ions/readme.txt>, accessed Aug 2004).
- Ogilvie, K.W., J.D. Scudder, and M. Sugiura, Electron energy flux in the solar wind, *J. Geophys. Res.*, 76, 8165, 1971.
- Ogilvie, K.W., and M.A. Coplan, Solar wind composition, in U.S. National Report to IUGG, 1991-1994, *Rev. Geophys.*, Vol. 33 Suppl., American Geophysical Union, 1995.
- Pilipp, W.G., et al., Characteristics of electron velocity distribution functions in the solar wind derived from the Helios plasma experiments, *J. Geophys. Res.*, 92, 1075-1092, 1987.
- Scudder, J.D., On the causes of temperature change in inhomogeneous low-density astrophysical plasmas, *Astrophys. J.*, 398, 299-318, 1992.